ACS OMEGA

http://pubs.acs.org/journal/acsodf

Article

Strategy of Electrolyte Design: Triethanolamine as a Polydentate Ligand to Improve Solvation of Zinc in Zinc−Air Batteries

Chenghua Wang, Huiyu Huang, Xueyan Sun, Xiaobin Deng, Yuan Lei, Wenbing Hao, Yilun Liu, Xi Chen, and Wei Zhao*

Cite This: *ACS Omega* 2023, 8, 8092−8100

Read Online

ACCESS | Metrics & More | Article Recommendations | Supporting Information

ABSTRACT: The zinc−air batteries (ZABs) are regarded as the most potential energy storage device for the next generation. However, the zinc anode passivation and hydrogen evolution reaction (HER) in alkaline electrolyte situations inhibit the zinc plate working efficiency, which needs to improve zinc solvation and better electrolyte strategy. In this work, we propose a design of new electrolyte by using a polydentate ligand to stabilize the zinc ion divorced from the zinc anode. The formation of the passivation film is suppressed greatly, compared to the traditional electrolyte. The characterization result presents that the quantity of the passivation film is reduced to nearly 33% of pure KOH result. Besides, triethanolamine (TEA) as an anionic surfactant inhibits the HER effect to improve the efficiency of the zinc anode. The discharging and recycling test indicates that the specific capacity of the battery with the effect of TEA is improved to nearly 85 mA h/cm^2 compared to 0.21 mA h/cm^2 in 0.5 mol/L KOH, which is 350 times the result of the blank group. The electrochemical analysis results also indicate that zinc anode self-corrosion is palliated. With density function theory, calculation results prove the new complex existence and structure in electrolytes by the data of the molecular orbital (highest occupied molecular orbital−lowest unoccupied molecular orbital). A new theory of multi-dentate ligand inhibiting passivation is elicited and provides a new direction for ZABs' electrolyte design.

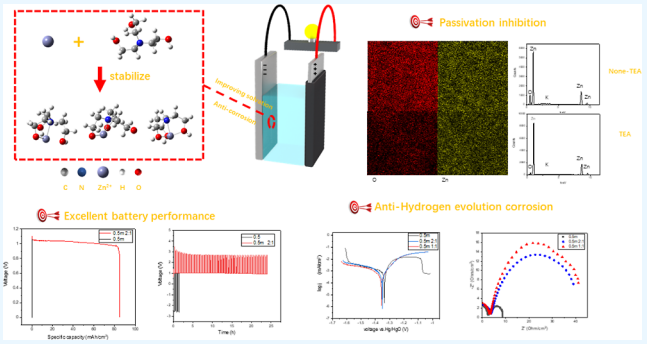

1. INTRODUCTION

With a trend of speeded-up electronic device development and a sharper energy situation, the need for advanced energy storage devices is becoming increasingly urgent.[1−3] The zinc−air batteries (ZABs) have attracted many scientists to work on them.[4,5] The ZABs are widely regarded as the next-generation energy election by their prominent potentiality in volumetric energy density (6136 W h L^{-1}) and specific capacity (1218 W h kg^{-1}), compared to lithium−air batteries. Therefore, many efforts of applying ZABs have been made in some small components, for example, emerging microelectronic devices powered by ZABs.[6,7] However, there still are unavoidable problems hindering the development of ZABs such as self-corrosion and passivation effect of the zinc anode.[8]

The formation of zinc oxide during working is one of the reasons that obstructs the ZABs' work by decreasing the utilization efficiency of zinc and diminishing battery life for a long time.[9] It has been revealed that zinc oxide generates an electrolyte during the ORR and aggregates into a film to cover the zinc anode.[10,11] Obviously, this kind of phenomenon causes impediments in continuous discharging because the film obstructs the zinc reaction with the electrolyte. For a long time, many scientists have done great work on the issue. Sun created a new system for the ZAB that zinc is transformed into peroxide and this kind of new electrolyte system can avoid the formation of ZnO to a certain extent.[12] Franke-Lang's work delivers the progress of comprehending the zinc anode, which proposes to use X-ray tomography technology to characterize the surface composition of the zinc anode.[13]

The hydrogen evolution reaction (HER) also called self-corrosion of zinc anode is another problem that bothers ZAB researchers, which is a parasitic reaction of the battery reaction. Many reports about doping some substance in the zinc anode to restrict HER were published. Most of them are rare earth metals, which are uneasy to practically apply for their toxicity and high price.[14−16] Besides, doping some things into the zinc anode decreases the zinc purity so that the amount of zinc per unit volume will be decreased. Apply surfactants to achieve some success in zinc vacancy battery electrolytes, where the

Received: December 23, 2022
Accepted: February 1, 2023
Published: February 14, 2023

choice of active agent is limited by the characteristics of the anchoring group.[17,18] What is more, another strategy is by using some additives into pure alkaline electrolytes such as ethanol and sodium dodecyl sulfate to hinder the HER, while these changes usually weaken the conductivity of electrolytes decreasing the concentration of KOH.[19,20]

Triethanolamine (TEA) as a polydentate N,O donor ligand can interact with different metal ions to form coordinate complexes. Kondratenko group synthesized and crystalized two new complexes containing zinc.[21−23] All these matters, this kind of zinc coordinates with TEA and can stably exist in solution. By interacting with TEA, the zinc ion is like wearing clothes and forms a bigger soluble atomic group. Inspired by this phenomenon, stable zinc ion coordination complexes can be created on purpose in ZAB systems to replace the former unstable zinc complexes ($[Zn(OH)_4]^{2-}$), which are easy to dehydrate to form the ZnO passivation film.

Here, we propose to use TEA in an aqueous ZAB electrolyte to create new zinc coordinate complexes in the electrolyte. Based on the mechanism of the passivation film, adding TEA plays a role in ligand interaction with zinc ions. The O and N atoms in TEA can provide electron pairs to zinc ion in its empty d orbit same as the OH^- ion which reduces the concentration of OH^- around the zinc. Meanwhile, a high concentration of OH^- causes dehydration and leads to ZnO formation.[9] Therefore, TEA as an additive can avoid the formation of the passivation film and improves the process of zinc solvation. Besides, for the effect of the anionic active agent from TEA, TEA also reduces the HER effect, which is confirmed by the Tafel plot. In the battery performance experiment, the ZAB involved TEA adding presents a higher area specific capacity (85 mA h/cm^2), which is 400 times the number in pure alkaline ZAB (0.2 mA h/cm^2). The result of the density functional theory (DFT) calculation proves that the TEA with the deprotonation state has a higher lowest unoccupied molecular orbital (LUMO) energy level (−0.1531 eV) than what OH^- has (−0.15843 eV) and close to the zinc highest occupied molecular orbital (HOMO) energy level (−0.09363 eV), which means that the combination between TEA and zinc is more stable than the one between hydroxide ion and zinc.

2. MATERIAL AND METHODS

2.1. Material and Electrode Preparation. The zinc metal used in this research is high-purity zinc foil (99.999%, 0.2 mm), which is cut into 13 × 50 and 10 × 10 mm^2 rectangle shapes for different work conditions. The electrolyte is made by dissolving KOH flakes (AR, Shanghai Macklin Biochemical Co., Ltd.) into deionized water whose conductivity is 18.25 MΩ/cm. The multidentate ligand used in the electrolyte is $TEA[N(CH_2CH_2OH)_3]$ (AR Shanghai Macklin Biochemical Co., Ltd.). The concentration of based KOH electrolyte is 0.5 mol/L, this concentration is relatively low and results in the formation of ZnO on the zinc anode, which simulates the passivation of the zinc anode. Because a high concentration of KOH will transfer zinc ions into $[Zn(OH)_4]^{2-}$, a less KOH existence environment causes a difficult transformation from $Zn(OH)_2$ to $[Zn(OH)_4]^{2-}$. Therefore, 0.5 mol/L based KOH electrolyte is selected. Moreover, the TEA concentration gradient is set by the mole ratio of KOH/TEA as 2:1 and 1:1.

2.2. Computer Calculation. For understanding the TEA working process and how it coordinates with zinc ions, the quantum chemistry calculation based on DFT was run on Gaussian 09W. First, the molecular model is imported into Gaussian 09W by Chem3D molecular files. Then, the structure of the molecule is optimized using Gaussian to obtain the most stable conformation. Finally, the results of molecular orbital calculations are obtained using the energy module. Solvent correction was added to all DFT calculations, and the solvent was water. The selection of relevant calculation methods is shown in Figure 1. After calculation, the information on molecule orbitals (MOs) was acquired.

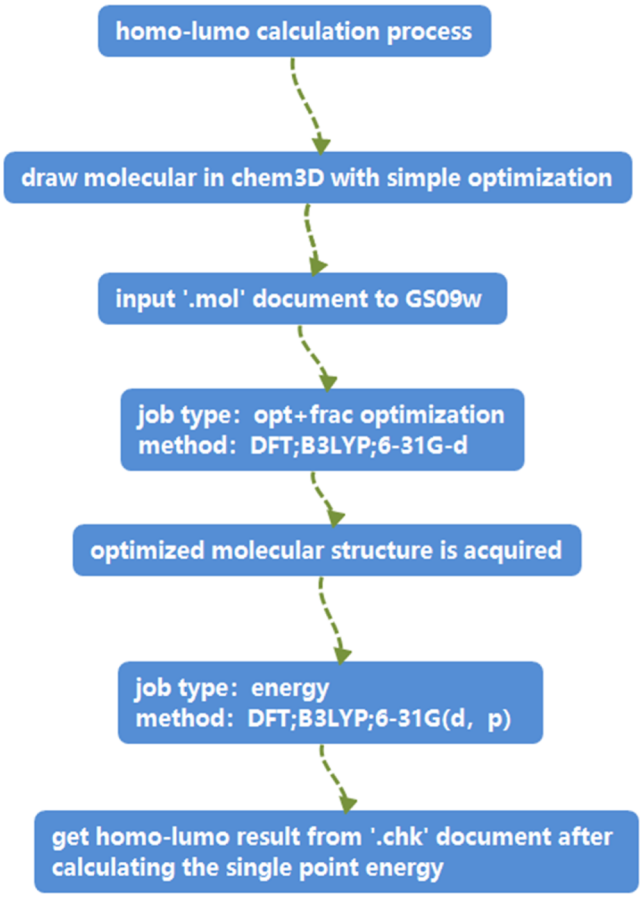

Figure 1. MOs calculation path and calculation method selection.

2.3. Electrochemical Measurements. On the electrochemical workstation (RST 5000), Tafel polarization and electrochemical impedance spectroscopy (EIS) plots were obtained. For the tests before, a three-electrode system was built, which contains a Hg/HgO (1 mol/L KOH R0501) reference electrode, a graphite counter electrode (10 × 10 × 5 mm^3), and a platinum electrode fixture, which can fix high purity zinc foil on it. The zinc foil is cut into a rectangle with 10 × 15 mm^2 so that the untouched area can be ensured 10 × 10 mm^2 and all the electrode fixtures with zinc foil as work electrodes. In addition, a two-electrode system consisting of two graphite electrodes is used to study the equivalent impedance of aqueous electrolytes. When testing is performed, the untouched area emerges under the level of electrolyte. Before assembling zinc foil with an electrode fixture, the zinc foil needs to be rinsed with deionized water and alcohol and dried by delicate task wipers (KIM tech). After a 30 min soaking of the electrolyte in a three-electrode system, the working electrode is ready for the EIS test. Besides, measuring

https://doi.org/10.1021/acsomega.2c08143
ACS Omega 2023, 8, 8092−8100

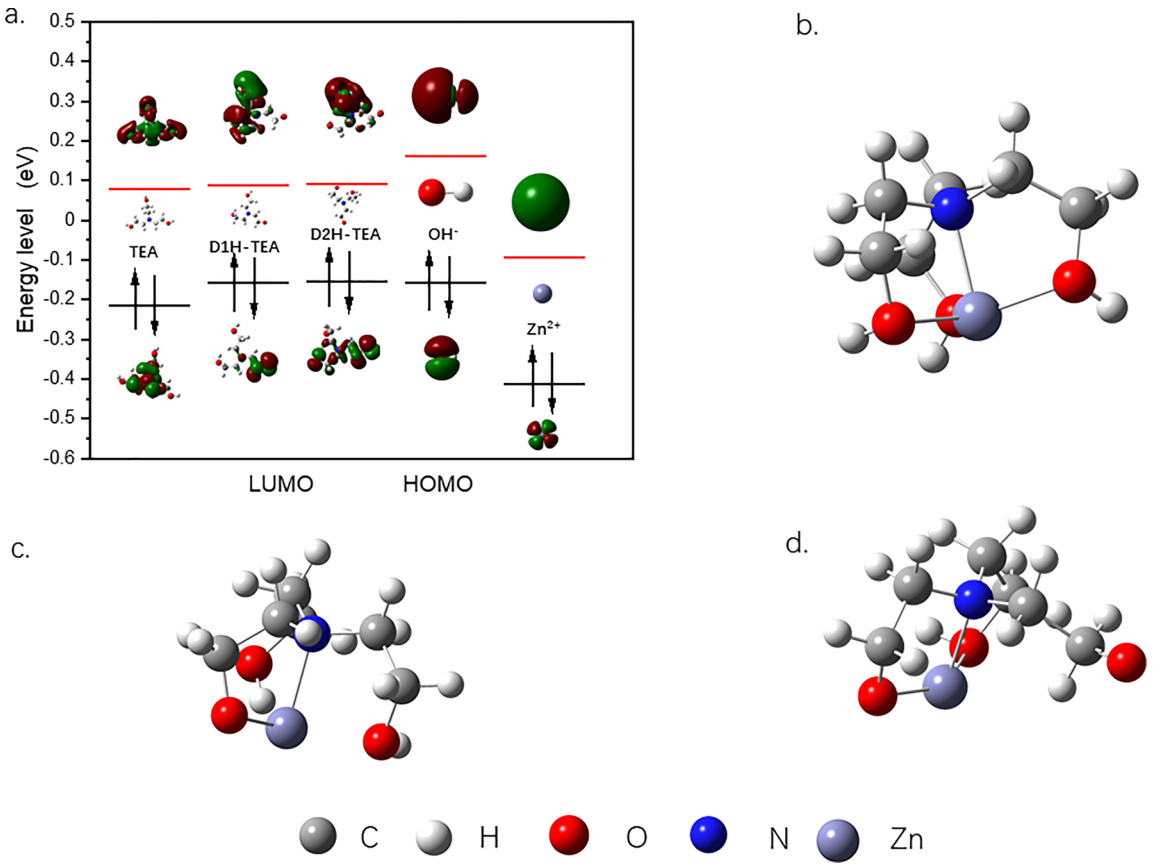

Figure 2. (a) MOs energy level distribution of different molecules, three different complex molecule structures: (b) TEA + Zn^{2+}, (c) TEA^{-} + Zn^{2+}, and (d) TEA^{2-} + Zn^{2+}.

frequency range was set from 100 000 to 0.1 Hz and the AC amplitude was 5 mV. The experiment parameters in EIS. The polarization was conducted from OCV ±0.3 V (vs Hg/HgO) and the scan rate is 5 mV/s. The Tafel polarization test was carried out after the EIS test. Every experiment was performed at room temperature.

2.4. Battery Performance Tests. The cathode of the ZAB was a kind of commercial film electrode (Metair Inc.), which uses MnO_2 as an ORR catalyst with a load of 3.5 mg/cm^2. The zinc anode is a 50 mm × 15 mm × 0.2 mm high-purity zinc foil. A plexiglass sandwich air battery module was used to carry out the discharge and discharge test, which holds about 30 mL electrolyte in the middle layer. Furthermore, the reaction area of this ZABs module is 1 cm^2. Figure S1 shows the detail of the battery. To study the power density of the battery, a linear voltammetric scan test from 1.5 to 0.2 V with a scan rate of 0.05 V/s was performed on the electrochemical workstation.

The battery capability test contains cycle ability and discharge experiment at room temperature. The discharge test is under the 5 mA/cm^2 to compare the TEA influence on discharge capability. During the cycle test, the experiment is arranged in discharging 5 mA/cm^2 for 15 min and charging 15 mA/cm^2 for 5 min.

2.5. Anode Surface Characterization. The zinc anode sample was collected after the discharge test furthermore the samples were syringed with deionized water and alcohol afterward. Finally, the zinc sample was cut into 15 × 15 mm^2 squares around the reaction area after a 10 min freeze-drying. The morphology of the zinc anode is investigated by scanning electron microscopy (SEM, Quanta 250 FEG). Besides, X-ray-energy-dispersive spectrometry (EDS), and mapping of (N, Zn, and O) was also covered. X-ray polycrystalline diffraction test (Bruker D8 ADVANCE) was also performed at a scan rate of 5°/min on the reaction surface of the zinc anode after discharge.

2.6. Electrolyte Characterization. After the discharge test, each batch of the ZAB electrolyte was almost gathered into sample tubes and put into a freeze dryer with a 12 h drying process. Later, the electrolyte crystal was received from the dryer. The Raman and Fourier transform infrared (FT-IR) test is carried out on the crystal.

3. RESULTS AND DISCUSSION

3.1. DFT Calculation. Gaussian 09 is used in calculating different molecules HOMO and LUMO and corresponding energy levels including TEA, deprotonated TEAs, and OH^{-} to get the result of the HOMO and LUMO energy level figure (Figure 2a). According to the calculation result, with the deprotonation effect of TEA, the HOMO levels of different molecule structures have a positive correlation with the number of lost protons, which conforms to the principle of the oxidation reaction. By comparing the energy level of different molecule structures. The TEA molecule and OH^{-} ion have a very close HOMO energy level, which may refer to hydroxyl from TEA. Furthermore, deprotonated 1 proton and 2 protons TEA (D1H-TEA and D2H-TEA) have higher HOMO energy levels than what the hydroxide ion has. This shows that the TEA with its deprotonated ions (TEAs) have similar power to give electrons or provide an electron pair easily. The zinc ions oxidized from the anode have an empty d

https://doi.org/10.1021/acsomega.2c08143
ACS Omega 2023, 8, 8092−8100

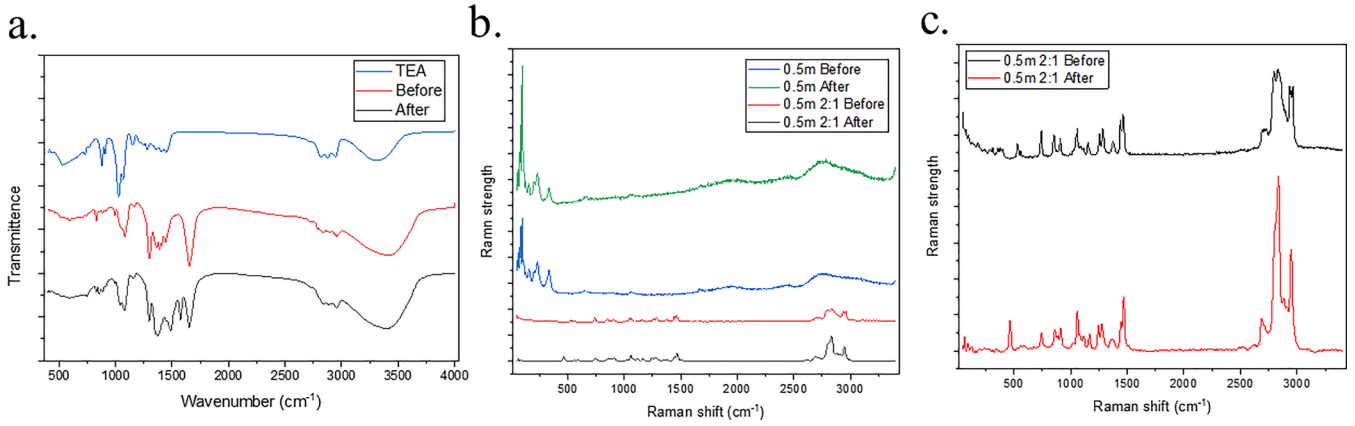

Figure 3. (a) FT-IR spectrum result of pure TEA, electrolyte crystal, and the after discharging, (b) total Raman spectrum result with four samples, and (c) Raman result from samples with TEA.

orbital, which is suitable for the electron pairs from N, and O atoms of the TEA molecule. Furthermore, it can be noticed that these molecules' HOMO energy level is close to the LUMO energy level of zinc ions. The closer HOMO and LUMO energy of different molecular means the reaction activation energy between two molecules is lower. According to previous research, TEA and its deprotonated status can coordinate with zinc ions, which occurred in the situation with methanol.[23] While the electrolyte used in ZAB is a water solution of hydroxide potassium, it means the proton is easy to be absorbed compared to the methanol in previous research. Therefore, the reaction of TEA deprotonation is promoted in the direction of losing proton. In other words, the environment of ZABs is suitable for TEA deprotonation. With this kind of promotion, the TEA is transformed into D1H-TEA and D2H-TEA which have higher HOMO energy levels than hydroxide ions. These deprotonated molecules will compete to combine with zinc ion lost electrons from the zinc anode against hydroxide ions because of the advantages of a higher HOMO energy level. Therefore, a new zinc coordination ion is produced in these factors.

The zinc coordination ion also is analyzed. Gaussian 09 is used to calculate and optimize the TEA, D1H-TEA, and D2H-TEA structure. The structure of these coordination cations is acquired from calculation results (Figure 2b–d). In summary, with the different deprotonation levels, their structure of them has a small difference. The differences concentrate on the combination method between the zinc ion and its multidentate ligands. In Figure 2b, the lone-pair electron from N and three O atoms in TEA enter the empty orbital of zinc ion, which are expressed in Gaussian as three new chemical bond formations referred coordination bonds. While in the deprotonated coordination situation, one of the three carbon chains from the N atom has no bond with the zinc ion. This phenomenon attributes to the increased electrostatic repulsion from the deprotonated oxygen and two oxygen from the other two legs. However, this feature can provide another advantage. In the reality solution environment, the deprotonated oxygen atom forms new hydrogen bonds with hydrogen atoms in electrolyte solutions such as OH^- and H_2O. With the hydron bond, small molecules in the electrolyte gather around the coordination ion, which increases the distance between the different zinc ions physically. Therefore, this kind of structure causes a form of zinc isolation from other zinc. Besides, the formation of zinc anode passivation layer ZnO is because the concentration of the zinc element reaches the critical value.[24] Compared to the $[Zn(OH)_4]^{2-}$ as a negative particle in traditional ZABs, the new complex ion is a positive polar particle. The positive charge carried by the new particles enables better solvation driven by the internal electric field because the internal electric field of ZABs is directed from the anode to the cathode. Hence, the process of zinc element concentration increasing is controlled so that the issue of formation passivation can be improved.

By calculating the HOMO and LUMO of zinc coordination ion, a MO picture is acquired. From the LUMO MO picture (Figure S2), it is noticed that the LUMO MO almost covers around the zinc part. The location of the LUMO orbital means for a new complex ion, the zinc is the most possible part of the molecule to get the electron. Specifically, when charging the battery, the zinc(II) in the complex can be reduced into a zinc atom. Meanwhile, the ligand of the complex, TEA, is released into the electrolyte after the zinc ion is reduced.

3.2. Electrolyte Crystal and Zinc Anode Characterization. *3.2.1. FT-IR and Raman Result.* Figure 3a shows FT-IR spectroscopy of pure TEA (AR) and the electrolyte freeze-dried crystallization mixture. The composition of the electrolyte mixture is a mole ratio of 2:1 (KOH/TEA). To investigate the electrolyte change, the samples are taken from discharging test before and after. First, the blue figure in FT-IR is the TEA pure sample result. It shows that TEA has three fingerprint peaks. The first is a strong absorption peak in the wavenumber range from around 1000 to 1300 cm^{-1} (s). These peaks attribute to the functional group existence of C–O stretch vibration.[25] Another group of significant peaks is located at a range from about 1451 cm^{-1} (m). These middle strong absorb peaks refer to the wagging vibration of C–H. Besides, a banding absorption peak can be noticed around 3300 cm^{-1} (b), which is from a stretch of –OH.

Compared to the electrolyte without discharging, the after-discharging result shows a red shift in 3300 cm^{-1} (b), which attributes to the –OH being stretched. Therefore, the chemical bond in –OH become weaker. It refers to the distance between oxygen and hydrogen atoms becoming longer. Besides, the absorb peak (s) around 1100 cm^{-1} appears a red shift. This phenomenon is caused by oxygen stretched away from the carbon atom in the C–O structure. With a coordination bond, the oxygen atom needs to combine with the zinc ion in the new site of hybrid orbital so that oxygen alienates the carbon atom, which weakens the bond C–O.

https://doi.org/10.1021/acsomega.2c08143
ACS Omega 2023, 8, 8092–8100

Lastly, the peaks in 1500 cm^{-1} (m) refer to the results of C−O vibration. It shows a blue shift result compared to the without-discharging result. The blue shift is caused by the pressed C−O bond because of the coordination between the zinc ion and oxygen.

Figure 3b is the summary result of the electrolyte crystal Raman spectrogram as a complement to the FT-IR result. The existence of TEA influences the shape of electrolyte crystals. The 0.5 m group shows a different shape with the group added TEA. However, before and after discharge showed similar shapes in general. Both present the same peaks in the same Raman shift. This is on account of the instability of complex ions formed by zinc ions with OH^- in the such concentration of OH^-. Therefore, the zinc(II) becomes ZnO passivation on the zinc anode, which results in the composition change of the electrolyte not being big after discharging. Based on this reason, both Raman diagrams are similar.

Figure 3c shows a detailed Raman result. At about 500 cm^{-1}, the after-discharging Raman result shows a new peak. This attributes to TEAs coordinated with the zinc ion.[22,26,27]

3.3. Anode and Electrolyte SEM. For further research on zinc anode discharging formation in different electrolytes, the zinc sample is acquired after discharging. The reaction area of zinc is observed under SEM to investigate the effect of the different electrolyte compositions. Figure 4a−d shows the

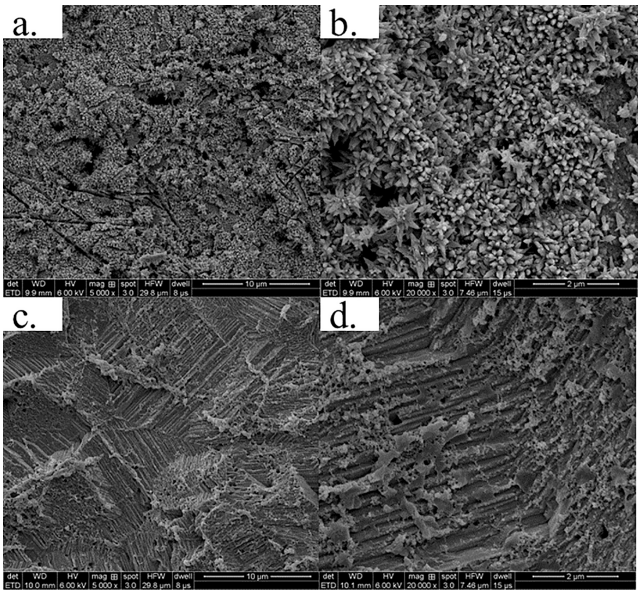

Figure 4. (a,b) Morphology picture of the pure KOH situation in magnification of 5000 and 20 000 and (c,d) morphology picture of the TEA group in magnification of 5000 and 20 000.

blank and the TEA group zinc morphology image in different magnification degrees. The image of the blank presents many clusters; moreover, spikes covered the core of them, which are clearer in the bigger magnification image. Meanwhile, in the TEA group, the zinc foil shows a different form. The electrochemical corrosion print is uniform; furthermore, the transition region shows a step-like pattern distributed in the transition part of different depths of the corrosion area.

In the discharging process of the blank, the zinc ion integrated with −OH in the electrolyte. Therefore, the intermediate products $[Zn(OH)_n^{2-n}]$ are formed. These matters form near the anode and are unstable. The instability means they cohere with each other and dehydrated.[18] The product of dehydration is ZnO. Hence, ZnO precipitated to form the solution of the cell and adhered to the surface of the anode so that a passivation film covers the zinc, which increases the internal resistance of the cell. The precipitated ZnO followed the law of nucleation.[28] While, during the discharging process, the dissolution of zinc is uneven in micro, which leads to some part of zinc bulging relatively. These convex parts are naturally nuclear for the precipitation of ZnO. Therefore, the image presents the clusters with spikes on the ground like coronavirus. However, the TEA group shows a smoother surface than the blank. During recycling, a glossy reaction area deters the formation of dendrites. When the TEA group discharges, the zinc is oxidized and dissolves into the electrolyte. The TEAs coordinate with the zinc ion as a ligand instead of OH^-. The newly formed complex ions are more stable than the $Zn(OH)_n^{2-n}$ as well as soluble, which allows the zinc element to exist in the solution. Therefore, the zinc ion gets rid of the fate of dehydration and is absorbed on the surface of the anode as ZnO.

The EDS and mapping of the anode reaction area also was performed to identify the discharging product on zinc foils. The tested kinds of elements are potassium, oxygen, and zinc, respectively. The mapping result is presented in Figure 5. According to Table 1, the elemental potassium concentration did not differ significantly between the two groups of samples. Compared with the blank group, the TEA group had much more signal points in the potassium mapping results, but the signal intensity is weaker. Meanwhile, for the element of oxygen, the blank has a higher density, which is noticed by dense red dots. It means the oxygen element on the surface of the sample from the blank is higher than what the TEA has. Based on the similar potassium density, the redundant part of oxygen is attributed to the ZnO passivation layer on the blank sample.

Furthermore, according to the result of X-ray EDS (Table 1), more quantified information about the elements is obtained.

According to the concentration of the element, the oxygen from the TEA group has been decreased to one-third of the blank. Besides, both groups have closed the element concentrations of Zn and K. The X-ray diffraction (XRD) test results (Figure S5) also show that the passivation layer is greatly suppressed under the influence of TEA. Therefore, the formation of ZnO is suppressed by the coordination effect of TEA.

For more detailed information on electrolytes from the TEA group, the electrolyte crystal was investigated by the way of element mapping. The crystal of discharged electrolyte from the TEA group was taken as the sample. In the element mapping result (Figure 6a), elements of nitrogen (Figure 6b), carbon (Figure 6c), and zinc (Figure 6d) are detected. The carbon and nitrogen are from TEA molecules. Therefore, the number of carbons is far more than nitrogen. To locate the TEA molecule by the nitrogen sites because a TEA molecule only has one N atom, the TEA is evenly distributed in the electrolyte. Furthermore, the distribution of zinc atoms is similar to what nitrogen has. It proves that the zinc atoms are coordinated with TEA so that zinc cannot aggregate to form the ZnO but stably exist in the electrolyte. For Figure 6c, it is obtained that the density of carbon atoms is very large compared to the other two elements. Therefore, a large number of carbon chains from TEA molecules may play the

https://doi.org/10.1021/acsomega.2c08143
ACS Omega 2023, 8, 8092−8100

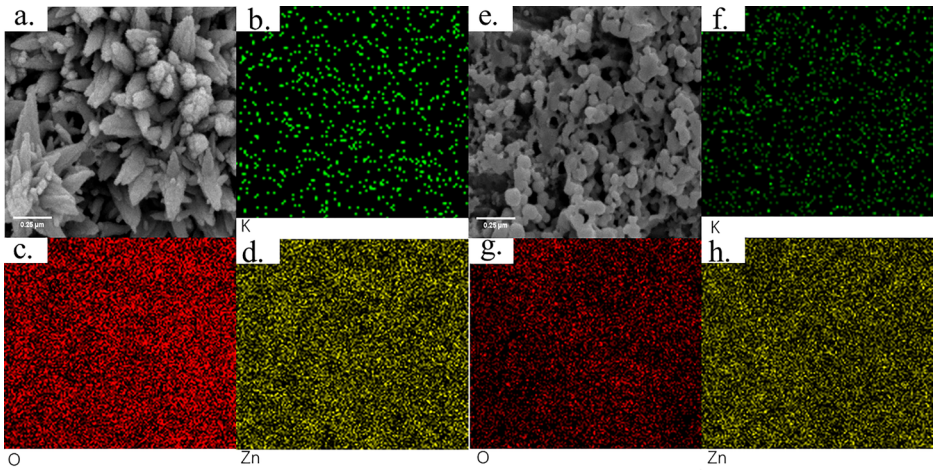

Figure 5. Mapping result of the blank group (a–d) and the TEA group (e–h), the origin SEM result (a,e), and the element result of potassium (b,f), oxygen (c,g), and zinc (d,h).

Table 1. X-ray EDS Result; B: The Blank Group; T: The TEA Group

element	concentration of element (%)	mass percentage (%)	atom percentage (%)
O (B)	5.98	22.98	54.91
K (B)	0.04	0.16	0.16
Zn (B)	17.13	76.85	44.93
O (T)	1.83	7.47	24.79
K (T)	0.01	0.05	0.07
Zn (T)	22.71	92.48	75.14

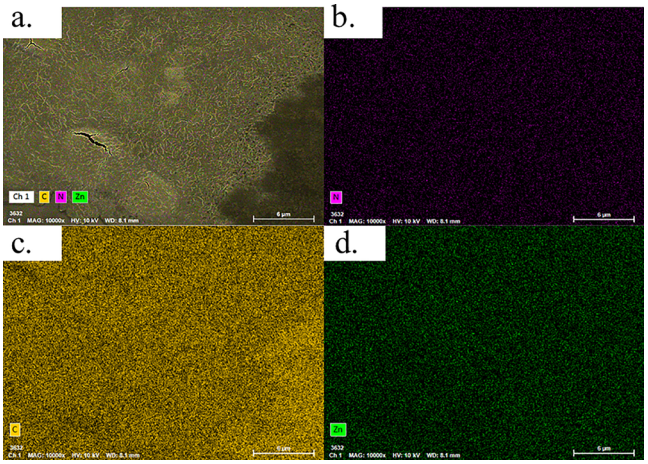

Figure 6. Electrolyte crystal mapping picture of summary (a) nitrogen (b), carbon (c), and zinc (d).

role of the buffer layer for zinc, which refers to the optimized configuration of complex ions from the former Gaussian calculation result.

4. ELECTROCHEMICAL TEST

4.1. Tafel Polarization. To figure out more detail about the TEA effect in the self-corrosion of the zinc anode, potentiodynamic polarization was performed. Figure 7a shows the Tafel plot of zinc anode in the solution of 0.5 mol/L KOH in different concentrations of TEA. Besides, Table 2 covers some relative parameters such as corrosion potential, corrosion current density, and other Tafel constants, acquired from the curve of the Tafel plot. In summary, the existence of TEA in different concentrations of KOH solution has a similar influence in suppressing the self-corrosion of the zinc anode. Each corrosion potential is shifted to the negative direction with the participation of TEA in varying degrees. The phenomenon of corrosion potential shifting negatively indicates that the TEA plays the role of cationic surfactant in inhibition.[29] In the electrolyte solution, the hydroxyl group of the hydrophilic part of the TEA will preferentially adsorb to the metal surface, while the alkane at the other end will form a hydrophobic layer, thus reducing the contact between water molecules and the zinc anode, forming a barrier and slowing down the occurrence of self-corrosion.[30−32] Besides, at the end of the three legs from the N atom of TEA, the hydroxyl groups can form hydrogen bonds with water molecules or TEA. The H_2O forming H_2 is sluggish with the molecule net made by TEA and H_2O. The energy barrier of cathodic reaction in corrosion is lifted by this process.

Table 2 presents the essential data from each group of the different added amounts of TEA. These show the degree of TEA in inhibiting self-corrosion. With the addition of TEA, the corrosion current and cathodic Tafel constant (β_c) were reduced to one-third and one-fourth of the data from blank. These results present that the TEA palliates the cathode corrosion reaction. Therefore, the participation of TEA in electrolytes also inhibits the self-corrosion of the zinc anode.

4.2. Electrochemical Impedance. For deeply investigating the TEA working mechanism, the electrochemical impendence spectrum was performed on the tri-electrode system. Figure S3 shows the full result of EIS and Figure 7b shows the result from the 1st to 55th points. Besides, the shape of the equivalent circuit elements as well as the detailed information of elements in the circuit is covered in Figure S4 and Table S1.

According to the EIS result, it can be noticed that the EIS figure is composed of two capacity radians. In Figure 7b, it shows a quarter radian and a $2/3\pi$ rad radian followed. After adding TEA, the radius of the second capacity radian was enlarged obviously. A bigger capacity radian radius shows that the capacitive resistance is enlarged. For the metal–air battery, the capacity as a circuit element in the equivalent circuit of the battery system indicates the metal corrosion status. The increased capacitive resistance of the capacitor components in

https://doi.org/10.1021/acsomega.2c08143
ACS Omega 2023, 8, 8092−8100

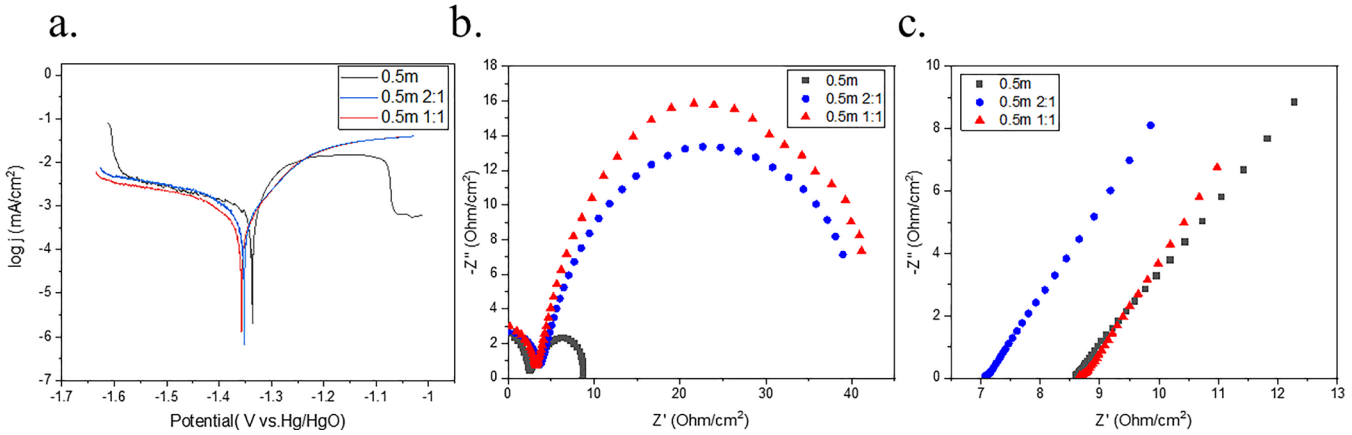

Figure 7. (a) Tafel polarization plot in different concentrations of TEA, (b) electrochemical AC impedance spectroscopy results of the zinc electrode in different TEA concentration electrolytes, and (c) AC impedance results of electrolytes with different TEA concentrations.

Table 2. Polarization Parameters for Zinc Anode

composition	E_{corr} (V)	I_{corr} (A/cm^2)	β_c (V/dec)
0.5m	−1.3263	6.3362×10^{-4}	0.168691
0.5m 2:1	−1.3373	2.260797×10^{-4}	0.100543
0.5m 1:1	−1.3528	2.161412×10^{-4}	0.044462

the equivalent circuit indicates an improvement in anti-corrosion.

Therefore, TEA plays a role in the anti-corrosion of zinc anode. For the full EIS figure (Figure S3), it also can be noticed that in the low-frequency area, due to the presence of TEA, the inductive radian has also changed. The inductance usually shows information about the adsorption of the electrode, which means that TEA changed the effect between the electrolyte and anode. It refers to the coordination effect between TEA and zinc.

The effect of TEA on the physical properties of the electrolyte was also investigated. The equivalent impedance of electrolytes with different compositions was tested using a two-electrode system (Figure 7c). The conductivity results are calculated from the equivalent impedance (Table S2). The TEA enhances the conductivity of the electrolyte at low concentrations and decreases it at high concentrations. For the battery, the high electrolyte conductivity helps to boost the battery current.

The viscosity of the electrolyte was tested for different compositions of electrolyte (Table S2). In general, the increase in TEA concentration increased the viscosity of the electrolyte. For the high concentration of TEA electrolyte, the viscosity (0.75 mPa·S) increases considerably, which confirms the lack of conductivity results at high concentrations.

4.3. Battery Performance Test. *4.3.1. Battery Discharge Test.* In the battery performance test, a sandwich-like ZAB is assembled by three pieces of plexiglass and a commercial cathode. The ZAB is discharged in the condition of 5 mA/cm^2 constant current density. Before accessing the circuit, ZAB is at a status of standstill for 30 min to let the electrolyte reach a steady state. All the cut-off voltage is set to 0 V to research the biggest capacity. The experiment electrolyte was composed of 0.5 mol KOH solution with a mole ratio of 2:1 compared to TEA.

According to Figure 8a, the specific capacity of TEA involved ZAB achieve a great improvement to 85 mA h/cm^2,

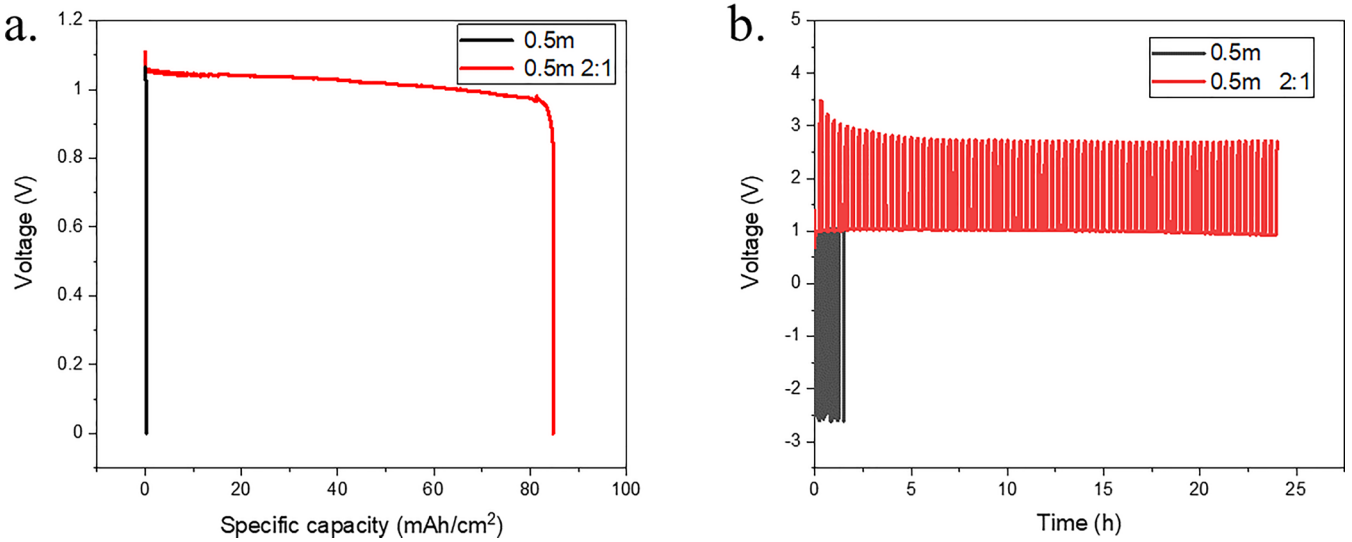

Figure 8. (a) Result of galvanostatic discharge and (b) part result of the recycling performance of ZAB with the discharging current 5 mA/cm^2 for 15 min and charging current 15 mA/cm^2 for 5 min per cycle.

https://doi.org/10.1021/acsomega.2c08143
ACS Omega 2023, 8, 8092−8100

compared to 0.21 mA h/cm^2 which the blank has. As mentioned before, in low concentrations of KOH, the effect of zinc passivation is augmented. Therefore, after discharging, the zinc anode got passivated quickly, which increases the internal resistance of ZAB. The ZAB without TEA has a quick passivation process, followed by increasing resistance rapidly. The output voltage got decreased by the internal resistance change. Therefore, the duration of the battery is reduced by the passivation process. Meanwhile, with adding TEA, the battery shows a much longer duration performance compared to blank. This immense gap between both performances attributes to the TEA changing path to passivation to postpone the zinc passivation.

4.3.2. Battery Cycle Test. Figure 8b shows parts of the battery cycle performance result (<24 h). According to the result, the blank group can not finish a single cycle because of the passivation effect. Therefore, the equipment detected a negative voltage of the battery. Therefore, the result shows that after a short period of discharging, the voltage of the battery reaches 0 V even negative. Meanwhile, for another group with TEA, the result shows good performance. In the first few cycles, the charging voltage is a little higher than the formers, which may be because the battery system is still unstable. Moreover, from the seventh cycle, the charging voltage is stabilized. According to the full cycle results (Figure S6), the cycles of the TEA group finished reached almost 100 cycles.

5. CONCLUSIONS

Generally, a kind of multidentate ligand compound, TEA, was researched on the aspect of inhibition of zinc passivation and self-corrosion in KOH electrolytes for ZABs. Benefiting from the complex structure formed by TEA and zinc, the process of zinc solvation is improved and thereby the passivation problem of zinc anode in aqueous ZABs is relieved. The zinc passivation is decreased to one-third of the blank, which increases the specific capacity of ZABs to 85 mA h/cm^2. DFT calculation and other characterization results verify the mechanism of action of TEA and indicated that with the use of a kind of multidentate ligand in ZAB, the zinc ion can be combined with the ligand to form a new relatively stable intermediate, which delays the formation of the anode passivation layer. In addition, the electrochemical analysis and other characterization results of TEA on the self-corrosion characteristics of the anode show that in addition to its coordination role, it also acts as an anionic surfactant to delay the self-corrosion of the anode and increases the utilization rate of zinc. In summary, TEA plays the role of the zinc ion stable agent in the electrolyte to deal with passivation and self-corrosion problems.

The multi-functionality of TEA as an additive to aqueous electrolytes, combined with its triple hydroxyl molecular structure, is expected to provide new ideas for the development of hydrogel electrolytes beyond aqueous electrolytes, thus helping the development of flexible ZABs. In addition, TEA is an excellent hydrogen bonding donor. Combining its advantage of stabilizing zinc ions with the great potential of eutectic solvent materials in electrolytes, the development of aqueous eutectic electrolytes based on TEA will also promote the research of ZABs.

ASSOCIATED CONTENT

Supporting Information

The Supporting Information is available free of charge at https://pubs.acs.org/doi/10.1021/acsomega.2c08143.

Optical images of ZABs, molecular orbitals of the complexes, complete EIS images of different electrolytes, equivalent circuit diagrams and fitting results, conductivity and viscosity results of different electrolytes, XRD test results of the zinc anode reaction region, complete cycle performance, and power density test results of the battery (PDF)

AUTHOR INFORMATION

Corresponding Author

Wei Zhao − *School of Chemical Engineering, Northwest University, Xi'an 710069, China;* orcid.org/0000-0003-1999-7712; Email: zhaowei3313@nwu.edu.cn

Authors

Chenghua Wang − *School of Chemical Engineering, Northwest University, Xi'an 710069, China;* orcid.org/0000-0002-1175-9018

Huiyu Huang − *Centre for Photonic Systems, Electrical Engineering Division, Department of Engineering, University of Cambridge, Cambridge CB3 0FA, U.K.*

Xueyan Sun − *School of Chemical Engineering, Northwest University, Xi'an 710069, China*

Xiaobin Deng − *School of Chemical Engineering, Northwest University, Xi'an 710069, China*

Yuan Lei − *School of Chemical Engineering, Northwest University, Xi'an 710069, China*

Wenbing Hao − *Shaanxi WuZhou Mining Company Limited, Xi'An 710024, China*

Yilun Liu − *State Key Laboratory for Strength and Vibration of Mechanical Structures, School of Aerospace, Xi'an Jiaotong University, Xi'an 710049, China*

Xi Chen − *Earth Engineering Center, Center for Advanced Materials for Energy and Environment, Department of Earth and Environmental Engineering, Columbia University, New York, New York 10027, United States;* orcid.org/0000-0002-8911-4172

Complete contact information is available at: https://pubs.acs.org/10.1021/acsomega.2c08143

Notes

The authors declare no competing financial interest.

ACKNOWLEDGMENTS

This work was supported from the School of Chemical Engineering, Northwest University, Shaanxi Coal Geology Group Co., Ltd. and Special Funds for Scientific and Technological Innovation of State-Owned Capital Operation Budget in Shaanxi Province. Support from the Natural Science Basic Research Program of Shaanxi (program no. 2023-JC-YB-046) and The Key Research and Development Program of Shaanxi (program no. 2022-LL-QYLH-00X).

REFERENCES

(1) Li, Y.; Dai, H. Recent advances in zinc-air batteries. *Chem. Soc. Rev.* **2014**, *43*, 5257−5275.

(2) Li, M.; Meng, J.; Li, Q.; Huang, M.; Liu, X.; Owusu, K. A.; Liu, Z.; Mai, L. Finely Crafted 3D Electrodes for Dendrite-Free and High-

Performance Flexible Fiber-Shaped Zn-Co Batteries. *Adv. Funct. Mater.* **2018**, *28*, 1802016.
(3) Qu, S.; Liu, B.; Fan, X.; Liu, X.; Liu, J.; Ding, J.; Han, X.; Deng, Y.; Hu, W.; Zhong, C. 3D Foam Anode and Hydrogel Electrolyte for High-Performance and Stable Flexible Zinc−Air Battery. *ChemistrySelect* **2020**, *5*, 8305−8310.
(4) Lu, Y.; Zou, S.; Li, J.; Li, C.; Liu, X.; Dong, D. Fe, B, and N Co-doped Carbon Nanoribbons Derived from Heteroatom Polymers as High-Performance Oxygen Reduction Reaction Electrocatalysts for Zinc-Air Batteries. *Langmuir* **2021**, *37*, 13018−13026.
(5) Wang, X.; Yang, Y.; Wang, R.; Li, L.; Zhao, X.; Zhang, W. Porous Ni_3S_2-Co_9S_8 Carbon Aerogels Derived from Carrageenan/NiCo-MOF Hydrogels as an Efficient Electrocatalyst for Oxygen Evolution in Rechargeable Zn-Air Batteries. *Langmuir* **2022**, *38*, 7280−7289.
(6) Neburchilov, V.; Wang, H.; Martin, J. J.; Qu, W. A review on air cathodes for zinc−air fuel cells. *J. Power Sources* **2010**, *195*, 1271−1291.
(7) Fu, J.; Cano, Z. P.; Park, M. G.; Yu, A.; Fowler, M.; Chen, Z. Electrically Rechargeable Zinc-Air Batteries: Progress, Challenges, and Perspectives. *Adv. Mater.* **2017**, *29*, 1604685.
(8) Tran, T. N. T.; Clark, M. P.; Xiong, M.; Chung, H.-J.; Ivey, D. G. A tri-electrode configuration for zinc-air batteries using gel polymer electrolytes. *Electrochim. Acta* **2020**, *357*, 136865.
(9) Baugh, L. M.; Higginson, A. Passivation of zinc in concentrated alkaline solution—I. Characteristics of active dissolution prior to passivation. *Electrochim. Acta* **1985**, *30*, 1163−1172.
(10) Amin, M. A. Passivity and passivity breakdown of a zinc electrode in aerated neutral sodium nitrate solutions. *Electrochim. Acta* **2005**, *50*, 1265−1274.
(11) Wang, R. Y.; Kirk, D. W.; Zhang, G. X. Effects of Deposition Conditions on the Morphology of Zinc Deposits from Alkaline Zincate Solutions. *J. Electrochem. Soc.* **2006**, *153*, C357.
(12) Sun, W.; Wang, F.; Zhang, B.; Zhang, M.; Küpers, V.; Ji, X.; Theile, C.; Bieker, P.; Xu, K.; Wang, C.; Winter, M. A rechargeable zinc-air battery based on zinc peroxide chemistry. *Science* **2021**, *371*, 46−51.
(13) Franke-Lang, R.; Arlt, T.; Manke, I.; Kowal, J. X-ray tomography as a powerful method for zinc-air battery research. *J. Power Sources* **2017**, *370*, 45−51.
(14) Wongrujipairoj, K.; Poolnapol, L.; Arpornwichanop, A.; Suren, S.; Kheawhom, S. Suppression of zinc anode corrosion for printed flexible zinc-air battery. *Phys. Status Solidi B* **2017**, *254*, 1600442.
(15) Perez, M. G.; O'Keefe, M. J.; O'Keefe, T.; Ludlow, D. Chemical and morphological analyses of zinc powders for alkaline batteries. *J. Appl. Electrochem.* **2007**, *37*, 225−231.
(16) Devyatkina, T. I.; Gun'ko, Y. L.; Mikhalenko, M. G. Development of ways to diminish corrosion of zinc electrode. *Russ. J. Appl. Chem.* **2001**, *74*, 1122−1125.
(17) Hosseini, S.; Lao-atiman, W.; Han, S. J.; Arpornwichanop, A.; Yonezawa, T.; Kheawhom, S. Discharge Performance of Zinc-Air Flow Batteries Under the Effects of Sodium Dodecyl Sulfate and Pluronic F-127. *Sci. Rep.* **2018**, *8*, 14909.
(18) Zhao, Z.; Fan, X.; Ding, J.; Hu, W.; Zhong, C.; Lu, J. Challenges in Zinc Electrodes for Alkaline Zinc−Air Batteries: Obstacles to Commercialization. *ACS Energy Lett.* **2019**, *4*, 2259−2270.
(19) Mainar, A. R.; Colmenares, L.; Grande, H.-J.; Blázquez, J. Enhancing the Cycle Life of a Zinc−Air Battery by Means of Electrolyte Additives and Zinc Surface Protection. *Batteries* **2018**, *4*, 46.
(20) Hosseini, S.; Han, S. J.; Arponwichanop, A.; Yonezawa, T.; Kheawhom, S. Ethanol as an electrolyte additive for alkaline zinc-air flow batteries. *Sci. Rep.* **2018**, *8*, 11273.
(21) Topcu, Y.; Yilmaz, V. T.; Thöne, C. Bis(triethanolamine-N,O,O′)zinc(II) disaccharinate. *Acta Crystallogr., Sect. E: Struct. Rep. Online* **2001**, *57*, m600−m602.
(22) Kar, M.; Winther-Jensen, B.; Forsyth, M.; MacFarlane, D. R. Exploring zinc coordination in novel zinc battery electrolytes. *Phys. Chem. Chem. Phys.* **2014**, *16*, 10816−10822.
(23) Kondratenko, Y.; Fundamensky, V.; Ignatyev, I.; Zolotarev, A.; Kochina, T.; Ugolkov, V. Synthesis and crystal structure of two zinc-containing complexes of triethanolamine. *Polyhedron* **2017**, *130*, 176−183.
(24) Yang, H. Improved discharge capacity and suppressed surface passivation of zinc anode in dilute alkaline solution using surfactant additives. *J. Power Sources* **2004**, *128*, 97−101.
(25) Anandhan, K.; Thilak Kumar, R. Synthesis, FTIR, UV-Vis and Photoluminescence characterizations of triethanolamine passivated CdO nanostructures. *Spectrochim. Acta, Part A* **2015**, *149*, 476−480.
(26) Jin, M.; He, G.; Zhang, H.; Zeng, J.; Xie, Z.; Xia, Y. Shape-controlled synthesis of copper nanocrystals in an aqueous solution with glucose as a reducing agent and hexadecylamine as a capping agent. *Angew. Chem., Int. Ed. Engl.* **2011**, *50*, 10560−10564.
(27) Karabach, Y. Y.; Kirillov, A. M.; Haukka, M.; Kopylovich, M. N.; Pombeiro, A. J. Copper(II) coordination polymers derived from triethanolamine and pyromellitic acid for bioinspired mild peroxidative oxidation of cyclohexane. *J. Inorg. Biochem.* **2008**, *102*, 1190−1194.
(28) Stamm, J.; Varzi, A.; Latz, A.; Horstmann, B. Modeling nucleation and growth of zinc oxide during discharge of primary zinc-air batteries. *J. Power Sources* **2017**, *360*, 136−149.
(29) Liu, Y.; Zhang, H.; Liu, Y.; Li, J.; Li, W. Inhibitive effect of quaternary ammonium-type surfactants on the self-corrosion of the anode in alkaline aluminium-air battery. *J. Power Sources* **2019**, *434*, 226723.
(30) Li, X.; Deng, S.; Fu, H. Inhibition by tetradecylpyridinium bromide of the corrosion of aluminium in hydrochloric acid solution. *Corros. Sci.* **2011**, *53*, 1529−1536.
(31) Abdel-Gaber, A. M.; Khamis, E.; Abo-Eldahab, H.; Adeel, S. Novel package for inhibition of aluminium corrosion in alkaline solutions. *Mater. Chem. Phys.* **2010**, *124*, 773−779.
(32) Hirai, T.; Yamaki, J.; Okada, T.; Yamaji, A. Inhibiting effects of Al corrosion by polymer ammonium chlorides in alkaline electrolyte. *Electrochim. Acta* **1985**, *30*, 61−67.

https://doi.org/10.1021/acsomega.2c08143
ACS Omega 2023, 8, 8092−8100